Desalination and Water Treatment
www.deswater.com

doi: 10.5004/dwt.2020.25963

197 (2020) 413–423
September

Shrimp shell (*Metapenaeus monoceros*) waste as a low-cost adsorbent for metanil yellow dye removal in aqueous solution

Putri Ramadhani[a], Zulkarnain Chaidir[b], Zilfa[c], Zebbil Billian Tomi[a], Disza Rahmiarti[a], Rahmiana Zein[a,*]

[a]*Laboratory of Analytical Environmental Chemistry, Department of Chemistry, Andalas University, Padang 25163, West Sumatera, Indonesia, Tel. +62751-71671; Fax: +62751-73118; emails: mimiedison@yahoo.co.id/rzein@sci.unand.ac.id (R. Zein), putrichem94@gmail.com (P. Ramadhani), bzebbil@yahoo.com (Z.B. Tomi), diszara@gmail.com (D. Rahmiarti)*
[b]*Laboratory of Biochemistry, Department of Chemistry, Andalas University, Padang 25163, West Sumatera, Indonesia, Tel. +62751-71671; Fax: +62751-73118; email: zulkarnainchaidir@sci.unand.ac.id (Z. Chaidir)*
[c]*Laboratory of Applied Chemistry, Department of Chemistry, Andalas University, Padang 25163, West Sumatera, Indonesia, Tel. +62751-71671; Fax: +62751-73118; email: zilfa@sci.unand.ac.id (Zilfa)*

Received 23 October 2019; Accepted 8 April 2020

ABSTRACT

Utilization of shrimp shell (*Metapenaeus monoceros*) to adsorb metanil yellow (MY) dye has been investigated using a batch system. The optimum conditions were achieved at pH 5, initial concentration 800 mg L^{-1}, contact time 75 min, the heating temperature of adsorbent 120°C, adsorbent mass 0.05 g, and particle size 25 μm. These parameters resulted in an adsorption capacity of 69.307 mg g^{-1}. The shrimp shell was characterized using Fourier-transform infrared spectroscopy, X-ray fluorescence spectroscopy, scanning electron microscopy energy-dispersive X-ray, and Brunauer–Emmett–Teller before and after the adsorption processes. Equilibrium adsorption data fitted a Langmuir isotherm model with R^2 = 0.9816 indicating chemical adsorption with a homogeneous biosorption process of the adsorbate onto a biosorbent surface forming a monolayer. The adsorption process followed pseudo-second-order kinetics with R^2 = 0.9953. The adsorption of MY onto the shrimp shell was an endothermic (positive $\Delta H°$) and non-spontaneous (positive $\Delta G°$) reaction. The reaction disorder was found to increase (positive $\Delta S°$). This study revealed that the shrimp shell was an effective low-cost adsorbent to remove MY dye.

Keywords: Shrimp shell; Adsorption; Metanil yellow; Isotherm; Kinetic; Thermodynamic

1. Introduction

Uncontrolled industrial activities discharge various hazardous materials into the environment including azo dyes which are widely used in textile, paper, plastic, and leather processing. These industries often release high concentrations of these toxic azo dyes in wastewater. One azo dye commonly used as colorant for nylon, wool, and silk is metanil yellow (MY) also known as Acid Yellow 36 (C.I. 13065). This is a water-soluble anionic and mono-azo dye that contains an azo group (–N=N–) [1]. MY is non-biodegradable even at low concentrations. The azo group in its structure makes the dye light resistant and it blocks sunlight and oxygen from penetrating to deeper levels of waterways and prevents the photosynthesis of aquatic plants. It is harmful to the environment especially aquatic life and can cause allergies, skin irritation, renal dysfunction, liver, brain, reproduction, and nervous system damage in humans [2].

* Corresponding author.

Various methods to chemically and physically remove the dye in an aqueous solution such as degradation [3], photolysis [4], coagulation and precipitation [5], photo-oxidation [6], membrane separation [7], and adsorption [8] have been reported [9]. One simple environmentally friendly method of waste treatment is adsorption. This method is most widely used because it is safe, simple, low-cost, efficient, and the absorbent can be recycled. Currently, biosorption methods are being developed that employ natural adsorbents derived from plants and animals (biosorbent) such as agricultural waste. These can have the advantage of high efficiency and biosorbents can be easy to obtain but their reuse in this way can effectively reduce solid organic waste [2,10]. Previous studies have investigated the ability of various biosorbents in such as apricot stones [11], cocoa shells [12], orange seeds [13], durian seeds [14], *Annona muricata* L seeds [15], rambutan seeds [2], fish bones [16], prawn shells [17] sago bark [18], and shrimp shells [19].

Shrimps are a marine species that are widespread and abundant. Shrimp shells, which make up about 40%–66% of shrimp weight are usually discharged as food waste and an industrial waste-product [20]. Previous research has shown that the calcium carbonate, chitin, and proteins shrimp shell mainly contained calcium carbonate, chitin, and proteins which will interact with dye molecules [21]. It might be an ideal candidate for environmentally friendly and low-cost adsorbents. Therefore, this study aimed to investigate the ability of shrimp shell as a low-cost adsorbent for removal MY in aqueous solution with the batch method. The influence of several parameters on adsorption such as pH, initial dye concentration, contact time, temperature, adsorbent mass, and particle size on the adsorption process was also studied. The equilibrium data were analyzed using Langmuir, Freundlich, Temkin, and Dubinin–Radushkevich adsorption isotherm models. The kinetic and thermodynamic parameters were studied as well in order to examine the adsorption mechanism.

2. Experimental setup

2.1. Materials

Shrimp shells (*Metapenaeus monoceros*) were obtained from the traditional market in Padang, West Sumatera, Indonesia. All reagents used are analytical grade purchased from Merck (Germany) and all solutions were prepared in distilled water.

2.2. Preparation of biosorbent

Shrimp shells were washed with water, dried at room temperature, crushed, and sieved. Then, the 25 g powder of shrimp shell was activated by soaking in 100 mL 0.01 M HNO_3 for 3 h, followed by washing with distilled water until neutral pH and then air-dried [22].

2.3. Dye solution preparation

A stock solution of 1,000 mg L^{-1} MY was prepared by dissolving 0.25 g of MY in 250 mL of distilled water. The standard solution was prepared by dilution MY at various concentrations (5–150 mg L^{-1}) [2].

2.4. Characterization of shrimp shell

The characterization of shrimp shell before and after biosorption process was examined using Fourier-transform infrared spectroscopy (FTIR, Unican Mattson Mod 7000 FTIR, United States), scanning electron microscopy energy-dispersive X-ray (SEM–EDX, Inspect F50, United States), X-ray fluorescence spectroscopy (XRF, PANalytical Epsilon 3, Netherlands) and Brunauer–Emmett–Teller (BET, Quantachrome QuadraSorb Evo, United States). The pH point of zero charges (pH_{pzc}) analysis was carried out by contacting 0.1 g of biosorbent with 50 mL of 0.1 M KCl. The pH was adjusted between 1–8 by adding either 0.01 M NaOH or 0.01 M HNO_3. The suspension was shaken for 24 h and the final pH (pH_f) of the supernatant was measured. The difference between the initial and final pH, ΔpH ($pH_f - pH_i$) was plotted against the initial pH (pH_i) and the intersection point resulted from the curve with vertical axis corresponded to the pH point of zero charges (pH_{pzc}) [23].

2.5. Biosorption studies

The biosorption process was conducted using a batch system. The effect of pH, concentration, contact time, temperature, adsorbents mass, and particle size was investigated. The experimental parameters were shown in Table 1. The pH of the solution was adjusted by adding 0.01 M HNO_3 or 0.01 M NaOH. The desired pH was maintained by a buffer solution. The Erlenmeyer was placed on a rotary shaker with agitation speed 100 rpm for 60 min. The solution was filtered from biosorbent using Whatman filter paper (No. 42). After that, the final concentration was determined by the UV-Vis spectrophotometer (Genesys 20 Thermo Scientific, Germany) at a wavelength of 435 nm. The adsorption capacity of the biosorbent (q, mg g^{-1}) and % removal was calculated by the following equation:

$$q = \frac{\left(C_0 - C_e\right)V}{m} \tag{1}$$

$$\%R = \frac{C_0 - C_e}{C_0} \times 100 \tag{2}$$

where C_0 and C_e were initial and equilibrium dye concentration in solutions (mg L^{-1}), respectively; V was the volume of the solution (L); m was the amount of biomass (g) [24].

2.6. Adsorption isotherm studies

The adsorption isotherm was a very important approach to illustrate how adsorbates are distributed between liquid and solid phases. In the present study, the Langmuir, Freundlich, Temkin, and Dubinin–Radushkevich isotherm models were used to describe the equilibrium biosorption data. Langmuir isotherm can be represented by the following equation:

$$\frac{1}{q_e} = \frac{1}{k_L q_m C_e} + \frac{1}{q_m} \tag{3}$$

Table 1
Experimental parameters of biosorption study of metanil yellow onto shrimp shell

No.	Parameter	Experimental parameters					
		Initial pH	Initial concentration (mg L^{-1})	Contact time (min)	Temperature (K)	Adsorbent mass (g)	Particle size (μm)
1	Initial pH	3–8	5	60	298	0.1	≤160
2	Initial concentration	5	60–1,200	60	298	0.1	≤160
3	Contact time	5	800	15–120	298	0.1	≤160
4	Temperature	5	800	75	363–483	0.1	≤160
5	Adsorbent mass	5	800	75	393	0.05–1.25	≤160
6	Particle size	5	800	75	393	0.05	≤25–≤425

where q_m was the maximum monolayer adsorption capacity of the adsorbent (mg g^{-1}), K_L was Langmuir adsorption constant (L mg^{-1}), q_e was the concentration of adsorbate on the adsorbent at equilibrium (mg g^{-1}) and C_e was the concentration of adsorbate in the solution at equilibrium (mg L^{-1}).

Langmuir adsorption isotherm has its own characteristic in determining the favorability of adsorption process that confirmed by calculating the dimensionless equilibrium parameter, usually known as separation factor (R_L) expressed by the following equation:

$$R_L = \frac{1}{1+\left(K_L \times C_0\right)} \tag{4}$$

where C_0 was initial concentration of adsorbate (mg L^{-1}). If $R_L > 1$, the adsorption process was unfavorable, if $0 < R_L < 1$, the adsorption process was favorable, if $R_L = 1$, the adsorption process was linear, while $R_L = 0$, the adsorption process was irreversible [25].

The Freundlich model equation was expressed by the following equation:

$$\log q_e = \log K_f + \frac{1}{n}\log C_e \tag{5}$$

where q_e was the amount of adsorbate on adsorbent at equilibrium (mg g^{-1}), C_e was the concentration of adsorbate in the solution at equilibrium (mg L^{-1}). K_f and n were Freundlich constant.

The equation of the Temkin adsorption isotherm model is as follows:

$$q_e = \beta \ln K_T + \beta \ln C_e \tag{6}$$

$$\beta = \frac{RT}{b} \tag{7}$$

where T is the absolute temperature (K), b is Temkin isotherm constant, R is the universal gas constant (8.314 J mol^{-1}), K_T is a constant related to the Temkin isotherm constant (L mg^{-1}), and β is the Temkin constant related to the heat of adsorption (J mol^{-1}).

The equation of the Dubinin–Radushkevich adsorption isotherm model is as follows:

$$\ln q_e = \ln q_m - K_{\mathrm{DR}}\varepsilon^2 \tag{8}$$

$$\varepsilon = RT \ln\left(\frac{C_e + 1}{C_e}\right) \tag{9}$$

$$E = \frac{1}{\sqrt{2K_{\mathrm{DR}}}} \tag{10}$$

where K_{DR} is a constant related to the mean free energy of adsorption (mol^2 J^{-1}), q_m is the theoretical maximum adsorption capacity (mg g^{-1}), ε is the Polyani potential (J mol^{-1}) and E is mean free energy of adsorption (kJ mol^{-1}).

3. Results and discussion

3.1. Characterization of shrimp shell

Characterization of shrimp shell with FTIR was performed in the wavenumber range of 4,000–400 cm^{-1}. The FTIR spectra analysis was important to identify the functional groups involved for adsorption of MY and to predict the adsorption mechanism between adsorbent and adsorbate.

Fig. 1 shows that there were various functional groups in the shrimp shell. The broad and strong peak at 3,266.26 cm^{-1} represented –OH stretching of the water molecule and N–H groups. The peak at 2,960.42 cm^{-1} could be assigned to C–H stretching and the peak around 1,912 cm^{-1} was related to C=O in amide. The peak at 2,302 cm^{-1} corresponds to –COOH group. The adsorption bands at 1,027.82 and 704.53 cm^{-1} were assigned to bending of C–N and N–H, respectively. The typical peaks representing CO_3^{2-} of the aragonite compound ($CaCO_3$) appear on the wavenumber 1,408.35 and 867.82 cm^{-1}. After the biosorption of MY, the peak of each functional group was shifted (Table 2). This indicated that the interaction between functional groups with MY molecules has occurred.

The biosorbent composition was changed after MY adsorption process (Table 3). The percentage of elements or oxides was decreased after adsorption processes such as Ca, P, CaO, P_2O_5, and others, indicated the presence of electrostatic interactions between the elements or oxides and the dye molecules. Aguayo-Villarreal et al. [26] have been reported about the calcium compounds in pecan shells are

responsible for the favorable adsorption of anionic dyes through the electrostatic interactions between the calcium cation of Pecan shells and the sulphonic groups of the dyes molecules, which would be dissociated in aqueous solution [26].

Fig. 2 shows the SEM's image of the biosorbent surface before and after the adsorption process took place. The biosorbent was activated by acid treatment before the adsorption process. Activation with 0.01 M HNO_3 aims to improve the specific surface area and porosity of adsorbent and to remove impurities so that the adsorption process can occur properly. The same results have been reported about activated red mud by acid treatment was highly efficient for the removal of methylene blue [27]. From Fig. 2a it can be seen that the surface of the biosorbent after activated by nitric acid has a rough surface, non-uniformly, and cavities. The existence of pore on the surface of biosorbent was proved by BET analysis. The BET analysis revealed that the average pore size of the shrimp shell was 1.273 Å. The pores and cavities act as a place for the adsorption site of MY so that the dye concentration in solution was decreased.

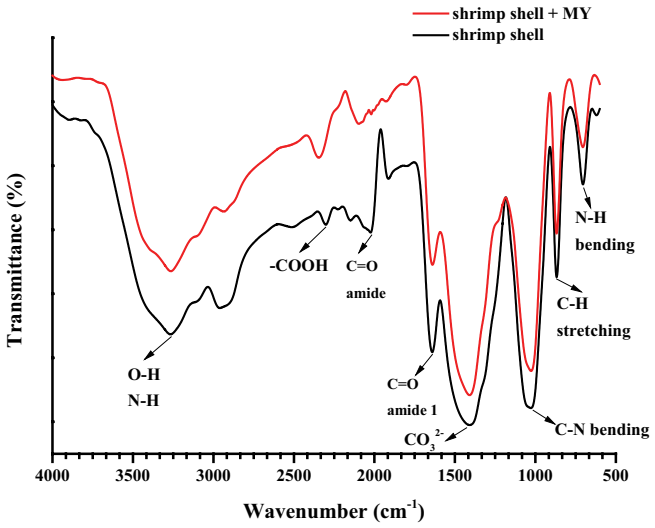

Fig. 1. FTIR spectra of shrimp shell before and after MY adsorption.

However, after the adsorption of MY, the surface of adsorbent was changed. Fig. 2b shows that MY molecules filled the pores and cavities, and then the surface becomes smoother due to the homogeneous layer of MY covering the biosorbent surface.

The specific surface area of the shrimp shell was 45.119 $m^2\ g^{-1}$, which showed that the biosorbent has a relatively large surface area. This value suggests that there was good feasibility of adsorbent to trap and absorb the dye molecules onto the surface biosorbent due to the high surface area that could provide more adsorption sites [28]. The results showed a decrease in the surface area of the shrimp shell after the absorption of MY dye from 45.119 to 33.079 $m^2\ g^{-1}$. This phenomenon proved that MY had covered the surface of the shrimp shell so that the surface area of the shrimp shell decreased, and the adsorption capacity increased.

EDX analysis of shrimp shell (Fig. 2) represented the number of elements Ca, P, Mg, O, N, and C. MY dye is a non-conductive compound so it does not appear in the EDX spectrum. After dye adsorption, the weight percent of carbon and oxygen elements increased from 9.42% and 33.45% to 11.24% and 41.62%, respectively. This proved the strong affinity of the adsorbent for the MY dye [29]. The affinity of adsorbent to adsorbate was indicated by separation

Table 3
XRF of shrimp shell before and after adsorption

Elements or oxides	% (w/w)	
	Before adsorption	After adsorption
Mg	2.485	2.018
P	7.614	7.019
Ca	85.443	85.013
Mn	0.035	0.024
Sr	1.927	1.462
MgO	3.437	2.777
P_2O_5	13.704	12.527
CaO	79.138	77.034
MnO	0.027	0.018
SrO	1.35	0.995

Table 2
Functional groups in shrimp shell

Functional groups	Before adsorption (cm^{-1})	After adsorption (cm^{-1})
OH–NH stretching	3,266.26	3,264.60
C–H stretching	2,960.42	2,835.39
–COOH	2,302	2,345.57
C=O in amide	1,912.82	–
C=O stretching in amide I	1,640.76	1,639.28
CO_3^{2-} (calcite)	1,408.35	1,408.73
C–N bending	1,027.82	1,026.45
CO_3^{2-} (calcite)/C–H stretching	867.82	868.36
N–H bending	704.53	704.91

factor value, R_L (Table 4). The value of the separation factor R_L is greater than 0 and less than 1, which suggested that the adsorption process is favorable [30]. The percentage of calcium and phosphor was decreased after MY adsorption indicated the adsorption process had taken place. This case was verified by the XRF analysis of adsorbent (Table 3) [15].

The determination of pHpzc value was important because it was related to the surface charge of the biosorbent that influenced the mechanism of MY adsorption. Adsorption of anions was favored at pH < pH_{pzc} while adsorption of cations was favored at pH > pH_{pzc} [31]. In Fig. 3 it can be seen that the pH_{pzc} value of the shrimp shell was 8.2. At this pH value, the shrimp shell has no positive or negative charge (zero charges). At pH > pH_{pzc} the shrimp shell has a negative charge that caused an electrostatic repulsion force between biosorbent surface and the MY molecules so that reduced adsorption capacity. While at pH < pH_{pzc} the surface of the shrimp shell has a positive charge that caused a strong electrostatic attraction between the surface of the shrimp shell with the MY molecules [31].

The MY contain a sulphonate group which exhibited anionic properties in an acidic medium so that the adsorption of the MY by the shrimp shell was predicted to be optimum

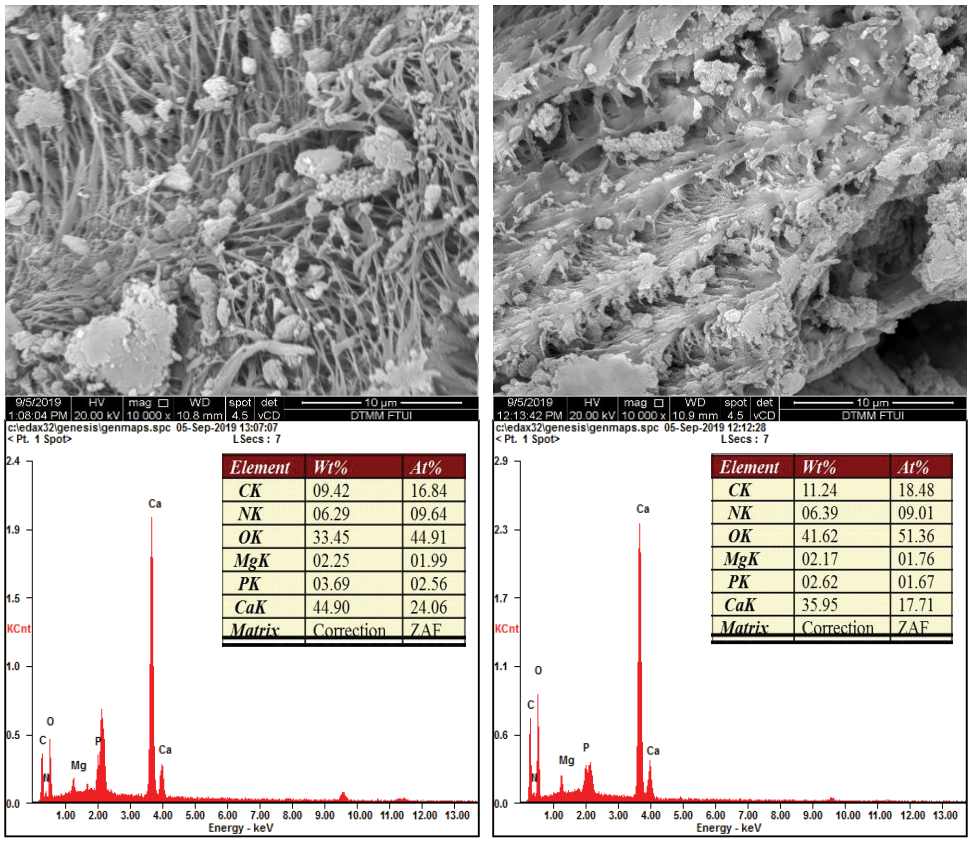

Fig. 2. (a) SEM–EDX of shrimp shell before sorption and (b) after metanil yellow dye sorption. (Magnification: 10,000 times).

Table 4
Isotherm model constant of Langmuir, Freundlich, Temkin, and Dubinin–Radushkevich on the adsorption of metanil yellow dye onto a shrimp shell

Langmuir				Freundlich		
q_m (mg g^{-1})	K_L (L mg^{-1})	R^2	R_L	K_f	1/n	R^2
44.62	0.005	0.981	0.141–0.767	0.845	0.590	0.906
Dubinin–Radushkevich				Temkin		
q_m (mg g^{-1})	K_{DR} (mol^2 g^{-1})	E (kJ mol^{-1})	R^2	K_T (L mg^{-1})	b	R^2
238.38	1.237×10^{-8}	4,040.40	0.586	0.029	12.305	0.823

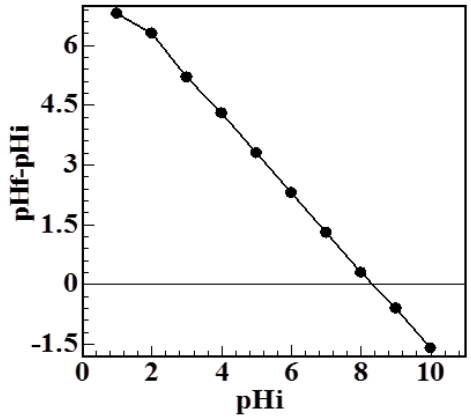

Fig. 3. pHpzc of shrimp shell.

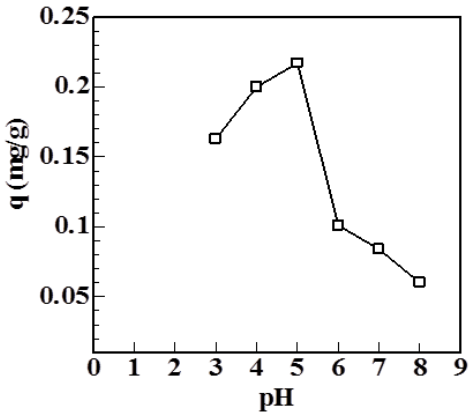

Fig. 4. Effect of pH on metanil yellow dye biosorption by shrimp shell. Experimental condition: concentration = 5 mg L^{-1}; biosorbent mass = 0.1 g; stirring speed = 100 rpm; contact time = 60 min; particle size = 160 μm.

at pH lower than 8.2. Several studies on the adsorption of anionic dye in the acidic medium by the fishery waste have been reported. Research conducted by Ribeiro et al. [16] showed the optimum adsorption of 5G reactive blue dye by fishbone occurred at pH below of pH_{pzc} (pH < 7.6).

3.2. Biosorption study

3.2.1. Effect of pH on adsorption capacity of MY

The effect of the pH of the dye solution was the most important factor that controlled the biosorption process. The pH of the system affected the surface properties of biosorbent and the mechanism of ionization or dissociation of dye molecules. In addition, the pH of the solution might also affect the electrostatic interaction between the surface of the biosorbent and the adsorbate molecules [2,15]. Effect of solution pH on the adsorption of MY onto shrimp shell was investigated within the range 3–8.

From Fig. 4 it can be seen that the optimum adsorption capacity was achieved at pH 5 with adsorption capacity of 0.217 mg g^{-1}. The adsorption capacity initially increased from 0.163 to 0.217 mg g^{-1} at pH 3–5. At the higher pH, the adsorption capacity decreased from 0.217 to 0.060 mg g^{-1} at pH 5 to 8. The pH of the solution strongly influenced the electrostatic interaction between the surface of the biosorbent and the dye molecule. At low pH, there was an increase of H^+ ions that will pull the electrostatic attraction force with the anionic dye so that the adsorption capacity increased. While at higher pH, the OH^- concentration increased. The presence of OH^- ions become a competitor that will compete with MY anions to fill the active site. So that the electrostatic repulsion existed between the positively charged surface of the biosorbent and anionic dye and decreased the adsorption capacity [32].

In the pH effect study, the optimum pH was achieved at pH 5. This was suitable with the pHpzc (pHpzc = 8.2), where in at pH < pHpzc the surface of the shrimp shell has more H^+ ions causing a strong electrostatic attraction between the surface of the shrimp shell with MY anion. Thus, the optimum adsorption of MY onto shrimp shells occurred at low pH. The same result has also reported by previous research [9].

3.2.2. Effect of concentration on adsorption capacity of MY

The effect of concentration of adsorbate was related to the liquid–solid adsorption process. The initial concentration of dye provided to transfer dye molecules between liquid and solid phases that affected the interaction between adsorbent and adsorbate [33]. The effect of MY concentration on the biosorption process was studied within the range 60–1,200 mg L^{-1}. Fig. 5 showed that the optimum adsorption of MY dye onto the shrimp shell was reached at the concentration of 800 mg L^{-1} with adsorption capacity 41.213 mg g^{-1}.

The adsorption capacity of shrimp shell increasing as the concentration increased. This phenomenon was affected by electrostatic interaction between MY molecules and the surface of the shrimp shell (active site). In addition, the adsorption capacity increased as the number of active sites available was sufficient to accommodate the amount of dye to be eliminated. The efficiency of dye removal depended on the initial dye concentration. The higher concentration will produce a higher driving force due to the concentration gradient. The driving force affected the speed of the diffusion of the dye from the solution to the biosorbent [2].

After the optimum concentration (800 mg L^{-1}), the adsorption capacity decreased because the number of active sites was not proportional to the amount of the dye, resulting in saturation of active site remaining the unabsorbed dye molecule [24,34]. A similar result has been reported for adsorption of MY by eggshell membrane showed an increase in concentration proportional to adsorption capacity [35].

The data was executed by several isotherm models. The adsorption isotherm was an important approach to illustrate how adsorbates are distributed between liquid and solid phases. The determination of the adsorption isotherm type aimed to determine the adsorption process that occurred between the shrimp shell as adsorbent and MY as adsorbate in equilibrium at a constant temperature [2].

Fig. 6 indicates that Langmuir isotherm was suitable to describe the adsorption process of MY onto the shrimp shell. This can be seen from a higher value of the coefficient

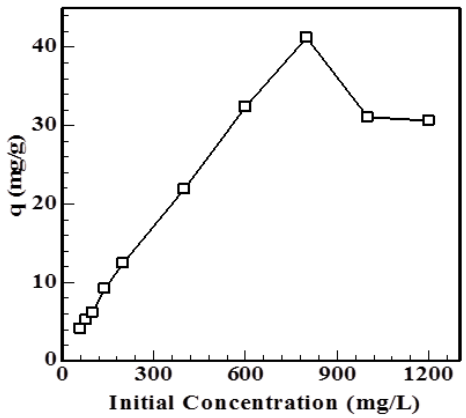

Fig. 5. Effect of initial concentration on the sorption capacity of metanil yellow dye on shrimp shell. Experimental condition: pH = 5; biosorbent mass = 0.1 g; stirring speed = 100 rpm; contact time = 60 min; particle size = 160 μm.

of determination (R^2) of the Langmuir isotherm linear equation (close to 1) compared to the Freundlich isotherm linear equation. This indicated that the process of MY biosorption occurred chemically through monolayer sorption with a homogenous surface of shrimp shell [31]. Similar results were also obtained by previous research [36].

The isotherm model constants of selected isotherm models can be seen in Table 4. These values were calculated from the slope and intercept of the linear equation of isotherm models.

In this present study, the R_L value ranges from 0.141 to 0.767. It was concluded that the process of adsorption of MY onto shrimp shell was favorable. Similar results were also obtained by previous research [25].

3.2.3. Effect of contact time and kinetics studies

The contact time effect was the time required to reach biosorption equilibrium. The effect of contact time on

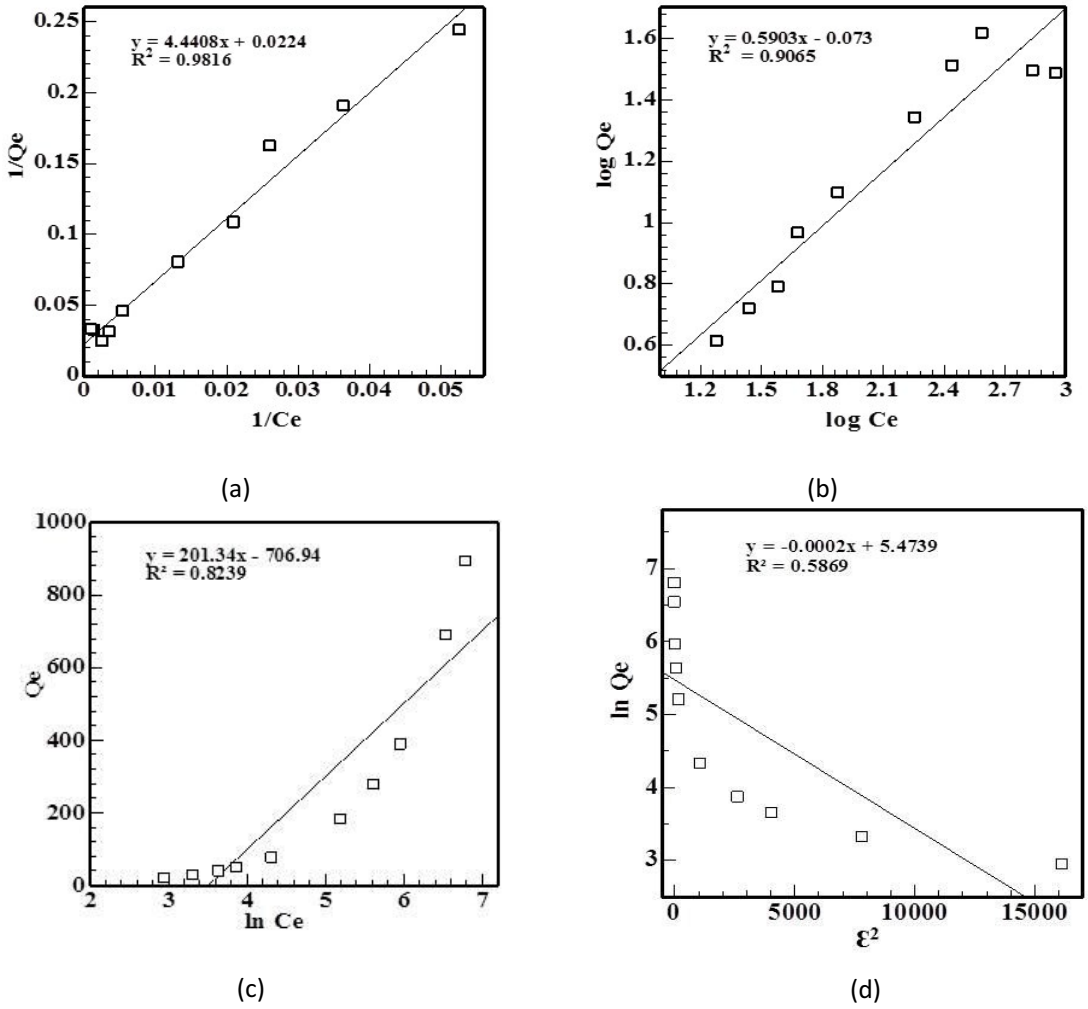

Fig. 6. (a) Langmuir, (b) Freundlich, (c) Temkin, and (d) Dubinin–Radushkevich isotherm linear equations for metanil yellow adsorption on shrimp shell.

the biosorption process was studied within the range of 15–120 min. Fig. 7 shows that the optimum adsorption of MY dye onto shrimp shell occurred at contact time 75 min with adsorption capacity 43.42 mg g^{-1}.

The increase in adsorption capacity was due to the longer collision time of the shrimp shell and the dye molecules so that the possibility of dye being adsorbed by the shrimp shell increased. This can be explained by the fact that the vacancy of active sites in shrimp shells so that the MY molecules easily interacted with the active site [37].

The kinetics study was evaluated using the pseudo-first-order and pseudo-second-order models. The kinetic parameters derived from these models were summarized in Table 5.

Fig. 8 shows that the kinetics of adsorption MY onto shrimp shell followed pseudo-second-order model indicated by determination coefficient (R^2) larger than pseudo-first-order. Also, the experimental q_e value (43.48 mg g^{-1}) was closed to the calculated q_e value from the pseudo-second-order model. It can be concluded that the adsorption process controlled by the chemisorption reaction between the shrimp shell and MY dye.

3.2.4. Effect of temperature on adsorption capacity of MY

The effect of heating temperature of adsorbent on the biosorption was studied within the range 90°C–210°C. Fig. 9 shows that the optimum adsorption of MY dye onto shrimp shell occurred at a heating temperature of adsorbent 120°C with adsorption capacity 57.838 mg g^{-1}.

Biosorbent heating aimed to determine the adsorbent's resistance to temperature and reduce the water content contained in shrimp shell powder so that the pores were open larger. This will cause interaction between the dye molecule and the biosorbent active site to begin optimally.

The thermodynamic parameters such as Gibbs free energy $\Delta G°$, enthalpy $\Delta H°$ and entropy $\Delta S°$ were calculated at different temperatures 298, 308, and 318 K by the following equations:

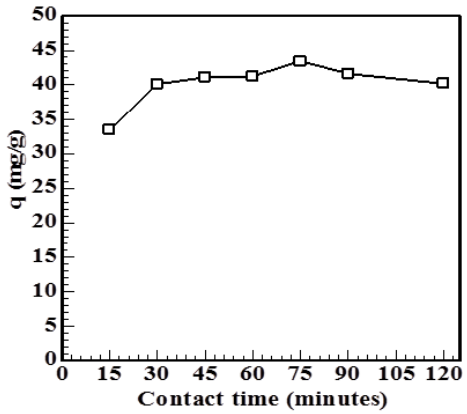

Fig. 7. Effect of contact time on the sorption capacity of metanil yellow on shrimp shell. Experimental condition: pH = 5; concentration = 800 mg L^{-1}; biosorbent mass = 0.1 g; stirring speed = 100 rpm; particle size = 160 μm.

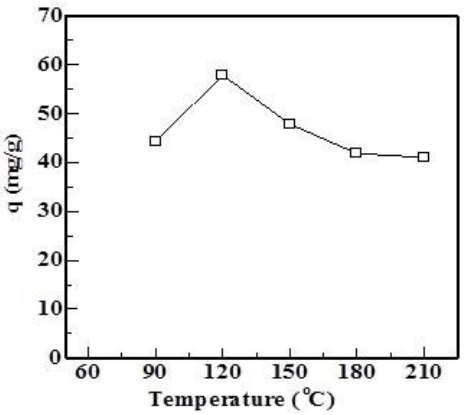

Fig. 9. Effect of heating temperature on the sorption capacity of metanil yellow on shrimp shell. Experimental condition: pH = 5; concentration = 800 mg L^{-1}; contact time = 75 min; biosorbent mass = 0.1 g; particle size = 160 μm; stirring speed = 100 rpm.

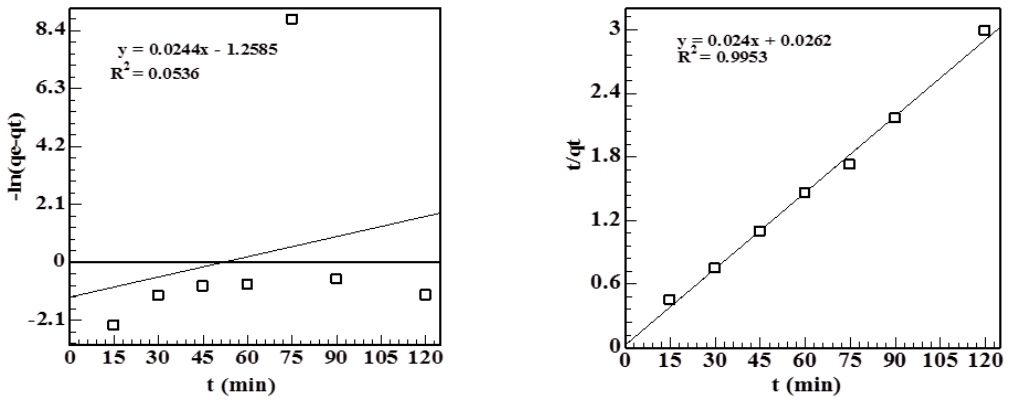

(a) (b)

Fig. 8. (a) Pseudo-first-order and (b) pseudo-second-order kinetic model for metanil yellow dye biosorption on shrimp shell.

$$\Delta G^\circ = -RT\ln K \quad (11)$$

$$K = \frac{\Delta S^\circ}{R} - \frac{\Delta H^\circ}{RT} \quad (12)$$

$$\Delta G^\circ = \Delta H^\circ - T\Delta S^\circ \quad (13)$$

where R is the universal gas constant, T (K) is the thermodynamic temperature, K is the adsorption equilibrium constant.

All the determined thermodynamic parameters are given in Table 6. The positive values of ΔG° and ΔH° at all studied temperatures indicated the non-spontaneous and endothermic reaction of MY dye adsorption process, respectively. The positive ΔS° values indicated a good affinity and increasing the degree of disorder at solid/solution interfered during the processes [38]. The same result has been reported by [36].

3.2.5. Effect of biosorbent mass on adsorption capacity of MY

Determination of biosorbent mass related to the biosorbent surface area and the availability of active sites. The effect of biosorbent mass on the biosorption was studied within range 0.05–1.25 g. Fig. 10 shows that the optimum adsorption capacity of MY dye onto shrimp shell was reached at biosorbent mass 0.05 g with adsorption capacity 66.007 mg g^{-1} and the removal percentage 97.5%.

From Fig. 10 it can be seen that as the adsorption capacity of MY dyes decreased as the number of adsorbents increased, but the percentage of removal increased significantly. It was related to a number of active sites on the surface of the adsorbent. The dye concentration remained constant, despite the fact that the number of adsorbents increased entirely so that the active site of the adsorbent becomes an unsaturated state because the dye molecules have no combine with it, this phenomenon leads to adsorption capacity reduction [36].

3.2.6. Effect of particle size on adsorption capacity of MY

The effect of particle size on the biosorbent was studied within range 25–425 μm. Fig. 11 shows that the optimum

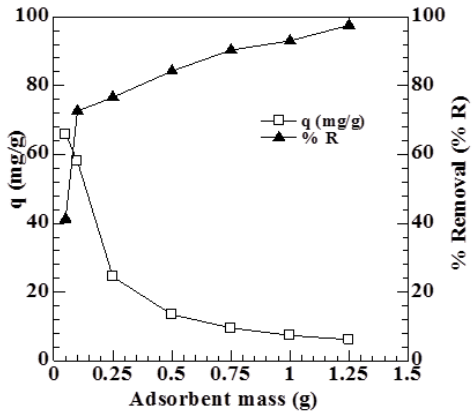

Fig. 10. Effect of biosorbent mass on the sorption capacity and % removal of metanil yellow on shrimp shell. Experimental condition: pH = 5; concentration = 800 mg L^{-1}; contact time = 75 min; stirring speed = 100 rpm; heating temperature = 120°C; particle size = 160 μm.

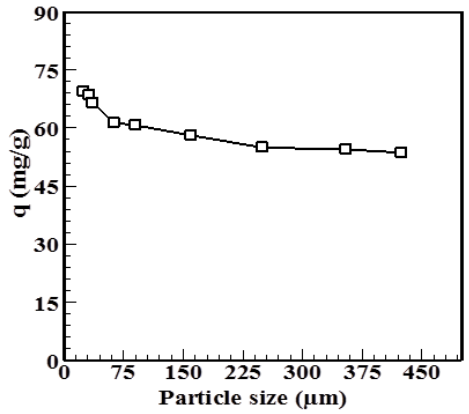

Fig. 11. Effect of particle size on the sorption capacity of metanil yellow dye on shrimp shell. Experimental condition: pH = 5; concentration = 800 mg L^{-1}; contact time = 75 min; stirring speed = 100 rpm; heating temperature = 120°C; biosorbent mass = 0.25 g.

Table 5
Kinetic parameters for metanil yellow removal using shrimp shell biosorbent

Pseudo-first-order			Pseudo-second-order		
K_1 (min^{-1})	q_e (mg g^{-1})	R^2	K_2 (min^{-1})	q_e (mg g^{-1})	R^2
0.0244	18.1342	0.0536	1.561×10^{-5}	41.66	0.9953

Table 6
Thermodynamic parameters for metanil yellow removal using shrimp shell biosorbent

Temperature (K)	ΔG° (kJ mol^{-1})	ΔH° (kJ mol^{-1})	ΔS° (kJ mol^{-1} K^{-1})
298	621.623		
308	14.154	5,877.2	18.002
318	261.574		

Table 7
Comparison of adsorption capacity of metanil yellow onto various adsorbents

Adsorbent	q (mg g^{-1})	Reference
Mg–Fe–NO_3 layered double hydroxide	42.72	[40]
Immobilized aquatic weed	9.91	[41]
Grafted palygorskite	47.03	[42]
HNO_3-treated-H_3PO_4-activated carbon (NATPAAC) from *Gmelina arborea*	2.35	[43]
Copper(II) oxide particles	3.22	[44]
Activated carbon from peanut shells	66.7	[45]
Shrimp shell	69.307	Present study

adsorption capacity of MY dye onto shrimp shell was reached at particle size 25 μm with adsorption capacity 69.307 mg g^{-1}.

The adsorption capacity of the biosorbent was decreased as the particle size increased. This phenomenon related to the surface area of the adsorbent. The small size of adsorbent was increased the surface area and the number of active sites for the adsorption process. A similar result has been reported by previous research [39].

The comparison of the adsorption capacity of MY on shrimp shell with other reported adsorbents was summarized in Table 7. It showed that the shrimp shell studied in this work has a large adsorption capacity for MY.

4. Conclusion

The shrimp shell (*Metapenaeus monoceros*) could be used to adsorb MY dye. The optimum conditions were achieved at pH 5, initial concentration 800 mg L^{-1}, contact time 75 min, the heating temperature of adsorbent 120°C, adsorbent mass 0.05 g, particle size 25 μm with adsorption capacity 69.307 mg g^{-1}. The characterization using FTIR, XRF, BET, and SEM–EDX showed the changes in the shrimp shell before and after the adsorption process. Equilibrium adsorption data were fitted to Langmuir isotherm (R^2, 0.981) indicating chemical adsorption and homogeneous biosorption process of adsorbate onto the biosorbent surface forming a monolayer. The adsorption process followed pseudo-second-order kinetics with R^2 0.995. The adsorption of MY dye onto the shrimp shell was an endothermic reaction with a non-spontaneous process. The reaction disorder was found to increase. This study was indicated that shrimp shells could be used as an effective low-cost adsorbent to remove MY dye.

Acknowledgments

The authors would like to thanks to Directorate for Research and Community Service, Directorate General of Strengthening for Research and Development, The Ministry of Research, Technology and Higher Education of the Republic of Indonesia who has funded this research in accordance with the letter assignment number: 051/SP2H/LT/DRPM/2019.

References

[1] P.K. Malik, Use of activated carbons prepared from sawdust and rice-husk for adsorption of acid dyes: a case study of acid yellow 36, Dyes Pigm., 56 (2003) 239–249.
[2] R. Zein, A.W. Astuti, D. Wahyuni, F. Furqani, Khoiriah, E. Munaf, Removal of methyl red from aqueous solution by *Neplhelium lappaceum*, Res. J. Pharm., Biol. Chem. Sci., 6 (2015) 86–97.
[3] P.S. Patil, Decolorization, degradation and kinetic study of textile dye navy blue HE2R using immobilized bacterial consortium PMB11, J. Environ. Sci. Pollut. Res., 2 (2016) 99–102.
[4] R. Zilfa, S. Upita, J. Novesar, M.L. Fajri, Utilization natural zeolyte from West Sumatera for TiO_2 support in degradation of congo red and a waste simulation by photolysis, Der Pharm. Lett., 9 (2017) 1–10.
[5] M.A. Sabur, A.A. Khan, S. Safiullah, Treatment of textile wastewater by coagulation precipitation method, J. Sci. Res., 4 (2012) 623–633.
[6] U.B. Deshannavar, A.A. Murgod, M.S. Golangade, P.B. Koli, B. Samyak, N.M. Naik, Photo-oxidation process – application for removal of color from textile industry effluent, Res. J. Chem. Sci., 2 (2012) 75–79.
[7] C. Thamaraiselvan, N. Michael, Y. Oren, Selective separation of dyes and brine recovery from textile wastewater by nanofiltration membranes, Chem. Eng. Technol., 41 (2018) 185–293.
[8] Y.Y. Wang, L.L. Zhu, X.H. Wang, W.R. Zheng, C. Hao, C.L. Jiang, J.B. Wu, Synthesis of aminated calcium lignosulfonate and its adsorption properties for azo dyes, J. Ind. Eng. Chem., 61 (2018) 321–330.
[9] S. Tural, T. Tarhan, B. Tural, Removal of hazardous azo dye metanil yellow from aqueous solution by cross-linked magnetic biosorbent; equilibrium and kinetic studies, Desal. Water Treat., 57 (2016) 13347–13356.
[10] R. Zein, R. Suhaili, F. Earnestly, Indrawati, E. Munaf, Removal of Pb(II), Cd(II) and Co(II) from aqueous solution using *Garcinia mangostana* L. fruit shell, J. Hazard. Mater., 181 (2010) 52–56.
[11] H.I. Albroomi, M.A. Elsayed, A. Baraka, M.A. Abdelmaged, Batch and fixed-bed adsorption of tartrazine azo-dye onto activated carbon prepared from apricot stones, Appl. Water Sci., 7 (2017) 2063–2074.
[12] M. Shanker, T. Chinniagounder, Adsorption of reactive dye using low cost adsorbent: Cocoa (Theobroma Cacao), World J. Appl. Environ. Chem., 1 (2012) 22–29.
[13] K. Jeyajothi, Removal of dyes from textile wastewater using Orange peel as adsorbent, J. Chem. Pharm. Sci., JCHPS Special Issue 4, December 2014.
[14] Z. Chaidir, D.T. Sagita, R. Zein, E. Munaf, Bioremoval of methyl orange dye using durian fruit (*Durio zibethinus*) Murr seeds as biosorbent, J. Chem. Pharm. Res., 7 (2015) 589–599.
[15] S. Fauzia, F. Furqani, R. Zein, E. Munaf, Adsorption and reaction kinetics of tatrazine by using *Annona muricata* L seeds, J. Chem. Pharm. Res., 7 (2015) 573–582.

[16] C. Ribeiro, F.B. Scheufele, F.R. Espinoza-Quiñones, A.N. Módenes, M.G.C. da Silva, M.G.A. Vieira, C.E. Borba, Characterization of *Oreochromis niloticus* fish scales and assessment of their potential on the adsorption of reactive blue 5G dye, Colloids Surf., A, 482 (2015) 693–701.
[17] T. Ravi, A.L. Stanley, G. Narendrakumar, A.K.S. Rao, Extraction of chitosan from prawn shell waste and its application in dye decolorization, J. Chem. Pharm. Res., 7 (2015) 695–703.
[18] S. Fauzia, H. Aziz, D. Dahlan, J. Namieśnik, R. Zein, Adsorption of Cr(VI) in aqueous solution using sago bark (*Metroxylon sagu*) as a new potential biosorbent, Desal. Water Treat., 147 (2019) 191–202.
[19] M. Fabbricino, L. Pontoni, Use of non-treated shrimp-shells for textile dye removal from wastewater, J. Environ. Chem. Eng., 4 (2016) 4100–4106.
[20] Y. Zhou, N. Fan, M. Xia, Adsorption of Congo red from aqueous solution onto shrimp shell powder, Adsorpt. Sci. Technol., 36 (2018) 1–21.
[21] S. Sawasdee, P. Watcharabundit, Effect of temperature on brilliant green adsorption by shrimp shell: equilibrium and kinetics, Chiang Mai Univ. J. Nat. Sci., 15 (2016) 221–236.
[22] R. Zein, S. Syukri, M. Muhammad, I. Pratiwi, D.R. Yutaro, The ability of Pensi (*Corbicula moltkiana*) shell to adsorb Cd(II) and Cr(VI) ions, AIP Conf. Proc., 2023 (2018) 020099-1–020099-8.
[23] M.C. Somasekhara Reddy, L. Sivaramakrishna, A. Varada Reddy, The use of an agricultural waste material, Jujuba seeds for the removal of anionic dye (Congo red) from aqueous medium, J. Hazard. Mater., 203–204 (2012) 118–127.
[24] Z. Chaidir, F. Furqani, R. Zein, E. Munaf, Utilization of *Annona muricata* L. seeds as potential adsorbents for the removal of rhodamine B from aqueous solution, J. Chem. Pharm. Res., 7 (2015) 879–888.
[25] A.A. Inyinbor, F.A. Adekola, G.A. Olatunji, Adsorption of Rhodamine B dye from aqueous solution on *Irvingia gabonensis* biomass: kinetics and thermodynamics studies, South African J. Chem., 68 (2015) 115–125.
[26] I.A. Aguayo-Villarreal, L.A. Ramírez-Montoya, V. Hernández-Montoya, A. Bonilla-Petriciolet, M.A. Montes-Morán, E.M. Ramírez-López, Sorption mechanism of anionic dyes on pecan nut shells (*Carya illinoinensis*) using batch and continuous systems, Ind. Crops Prod., 48 (2013) 89–97.
[27] Z.-P. Hu, Z.-M. Gao, X.Y. Liu, Z.-Y. Yuan, High-surface-area activated red mud for efficient removal of methylene blue from wastewater, Adsorpt. Sci. Technol., 36 (2018) 62–79.
[28] M.W. Ashraf, N. Abulibdeh, A. Salam, Adsorption studies of textile dye (*Chrysoidine*) from aqueous solutions using activated sawdust, Int. J. Chem. Eng., 2019 (2019) 8p, https://doi.org/10.1155/2019/9728156.
[29] K.Z. Elwakeel, A.M. Elgarahy, S.H. Mohammad, Use of beach bivalve shells located at Port Said coast (Egypt) as a green approach for methylene blue removal, J. Environ. Chem. Eng., 5 (2017) 578–587.
[30] X.H. Wang, C.L. Jiang, B.X. Hou, Y.Y. Wang, C. Hao, J.B. Wu, Carbon composite lignin-based adsorbents for the adsorption of dyes, Chemosphere, 206 (2018) 587–596.
[31] S. Sadaf, H.N. Bhatti, Batch and fixed bed column studies for the removal of Indosol Yellow BG dye by peanut husk, J. Taiwan Inst. Chem. Eng., 45 (2014) 541–553.
[32] T.S. Singh, Investigations on reduction of colour from pulp and paper mill effluent by activated coconut jute carbon, J. Water Supply Res. Technol. AQUA, 55 (2006) 57–64.
[33] J.M.F. Almeida, É.S. Oliveira, I.N. Silva, S.P.M.C. De Souza, N.S. Fernandes, Adsorption of Erichrome Black T from aqueous solution onto expanded perlite modified with orthophenanthroline, Rev. Virtual Quim., 9 (2017) 502–513.
[34] P.D. Saha, S. Chakraborty, S. Chowdhury, Batch and continuous (fixed-bed column) biosorption of crystal violet by *Artocarpus heterophyllus* (jackfruit) leaf powder, Colloids Surf., B, 92 (2012) 262–270.
[35] B.O. Isiuku, J.O. Onyeokoro, Batch biosorption of metanil yellow from aqueous solution on egg membrane: kinetics and mechanism, Int. J. Chem. Mater. Environ. Res., 5 (2018) 155–164.
[36] C.L. Jiang, X.H. Wang, D.M. Qin, W.X. Da, B.X. Hou, C. Hao, J.B. Wu, Construction of magnetic lignin-based adsorbent and its adsorption properties for dyes, J. Hazard. Mater., 369 (2019) 50–61.
[37] S. Boumchita, A. Lahrichi, Y. Benjelloun, S. Lairini, V. Nenov, F. Zerrouq, Application of peanut shell as a low-cost adsorbent for the removal of anionic dye from aqueous solutions, J. Mater. Environ. Sci., 8 (2017) 2353–2364.
[38] A. El-Imache, K. Ouazzani, The olive core, a promoter material for the adsorption of dyes: effects of certain parameters, kinetic and thermodynamic study, Orient. J. Chem. Int. Res. J. Pure Appl. Chem., 34 (2018) 2859–2866.
[39] E. Daneshvar, M.S. Sohrabi, M. Kousha, A. Bhatnagar, B. Aliakbarian, A. Converti, A.C. Norrström, shrimp shell as an efficient bioadsorbent for Acid Blue 25 dye removal from aqueous solution, J. Taiwan Inst. Chem. Eng., 45 (2014) 2926–2934.
[40] K. Nejati, Z. Rezvani, M. Mansurfar, A. Mirzaee, M. Mahkam, Adsorption of metanil yellow azoic dye from aqueous solution onto Mg-Fe-NO_3 layered double hydroxide, Zeitschrift Fur Anorg. Und Allg. Chemie., 637 (2011) 1573–1579.
[41] R. Sivashankar, V. Sivasubramanian, A.B. Sathya, S. Pallipad, Biosorption of Hazardous Azo Dye metanil yellow Using Immobilized Aquatic weed, Proc. of the Intl. Conf. on Future Trends in Structural, Civil, Environmental and Mechanical Engineering – FTSCEM 2013, Institute of Research Engineers and Doctors, Thailand, 2013, pp. 978–981.
[42] M.A. Moreira, K.J. Ciuffi, V. Rives, M.A. Vicente, R. Trujillano, A. Gil, S.A. Korili, E.H. de Faria, Effect of chemical modi fi cation of palygorskite and sepiolite by 3-aminopropyltriethoxisilane on adsorption of cationic and anionic dyes, Appl. Clay Sci., 135 (2016) 394–404.
[43] B.O. Isiuku, Batch removal of metanil yellow (MY) from aqueous solution by adsorption on HNO_3-treated-H_3PO_4-activated carbon (NATPAAC) from *Gmelina arborea* (*G. arborea*) bark: kinetic and mechanism studies, World News Nat. Sci., 13 (2017) 10–26.
[44] M.A. Ibrahim, M.B. Ibrahim, Adsorption of Alkali Blue, metanil yellow and Neutral Red dyes using copper(II) oxide particles: kinetic and thermodynamic studies, ChemSearch J., 9 (2018) 13–23.
[45] D.K. Garg, S. Sharma, C.B.K. Majumder, Application of waste peanut shells to form activated carbon and its utilization for the removal of Acid Yellow 36 from wastewater, Groundwater Sustainable Dev., 8 (2019) 512–519.